Author Response to Reviewer 1

Responses are shown in **blue**, and excerpts from the revised manuscript are shown in **red**.

> The manuscript presents an extension of previous work (Norooz Oliaee et al., 2022), advancing from instrument development toward field validation of UAV-based CH_4 flux estimation using controlled-release experiments. While the spectrometer design largely follows the earlier publication, the field deployment lacks a sufficiently rigorous assessment of the method under realistic conditions. In particular, the study does not include a systematic evaluation or quantification of uncertainties, biases, and errors related to interpolation approaches, instrumental performance, or atmospheric transport processes. With only two flights (of which just one was conducted under suitable wind conditions) the study does not provide valuable or generalizable insights for the reader.
>
> The paper may be suitable for publication after the authors address the concerns listed below.

We thank the reviewer for their detailed and thoughtful comments. We greatly appreciate their insights and their time in reviewing our work. We have incorporated the reviewer's feedback, and we feel that the revised manuscript is much stronger as a result.

The intent of this manuscript was to focus on the methane sensor miniaturization, a notable achievement that resulted in one of the smallest and lightest methane spectrometers reported to date. Compared with the previously published sensor (Norooz Oliaee et al., 2022), the new instrument is 84% smaller, 75% lighter, and consumes 40% less power. These improvements were achieved through the development of entirely new hardware and electronics, representing substantial changes to the overall design.

The controlled-release experiments were included to demonstrate the sensor's capability in the field rather than to provide an extensive validation dataset for statistical analysis. In addition to the two controlled-release experiments presented in this work, experiments were conducted on two additional measurement days. However, both additional days were characterized by highly variable wind direction (as defined by Morales et al. (2022)), which rendered the data unsuitable for flux estimation. As a result, only one flight day was conducted under sufficiently stable wind conditions for quantitative analysis. Results from one of these deployment days with unsuitable wind conditions were presented in the original manuscript to acknowledge the limitation of the method.

Though further controlled release experiments are beyond the scope of the present study, we agree with the reviewer that a more detailed discussion of uncertainties and limitations is needed. The manuscript has therefore been revised to include an expanded discussion of uncertainties, biases, and potential sources of error associated with the interpolation approach, instrumental performance, and atmospheric transport processes. These revisions clarify the limitations of the current dataset and place the presented results in the appropriate context. The changes are described in more detail below.

> **General comments:**
>
> Validation of plume-mapping and flux-estimation methods using sources with known emission rates has been extensively discussed in recent literature. Several studies (e.g., Andersen et al., 2021; Morales et al., 2022) present robust flight protocols and explicitly make clear suggestions for minimum wind speeds and other limiting factors that must be considered for appropriate quantitative flux analysis. These studies generally indicate optimal mean wind speeds of 2–6 m s^{-1}, while wind speeds <2 m s^{-1} lead to unreliable flux estimates due to large plume variability. The authors are encouraged to review this literature and use these recommendations into the design of future field campaigns.

We are familiar with the studies that the reviewer has referenced, and we acknowledge the value that these works have added to the literature. We also acknowledge that the omission of these citations in the original manuscript was an oversight, which has now been corrected. During field campaigns, we considered the findings of previous studies and we were aware that low wind speeds (<2.3 m s^{-1}) and high variability in wind direction (>33 degrees) can lead to unreliable flux estimates (Morales et al., 2022). The sensor was deployed in controlled release experiments on four measurement days. These campaigns required coordination with collaborators located in different regions (including the UAV operator) and advance reservation of the testing sites, which limited our ability to reschedule deployments when weather conditions were sub-optimal. As a result, three of the four measurement days were characterized by low or highly variable winds. If possible, future campaigns will be scheduled over a longer measurement period to increase the likelihood of obtaining suitable meteorological conditions.

> Existing flux-estimation methods, including mass-balance approaches (e.g., Morales et al., 2022) and Gaussian plume inversion modelling (e.g., Shah et al., 2020), typically show uncertainties ranging from ~17% to >200%, dominated by environmental conditions that control plume dispersion. Yet the present manuscript attributes its dominant uncertainty

solely to the extrapolation between the lowest flight transect and the ground. It is unclear why this assumption was not verified using a ground-based instrument (e.g., MIRA Pico Aeris) across the downwind plume (e.g. installed on a mobile platform such as a car).

We thank the reviewer for their observations. The uncertainty associated with extrapolating between the lowest flight transect and the ground arises primarily from uncertainty in the plume dispersion near the surface under varying environmental conditions. In this study, this extrapolation is significant because the highest methane mole fractions occurred in the lowest measured transects, and the plume dispersion between that transect and the ground is unknown. However, if the plume centre was higher off the ground such that the methane mole fractions in the lowest transect were near background levels, the extrapolation-related uncertainty would be negligible. In that scenario, uncertainty in plume dispersion would still be the dominant contributor. Accordingly, we have updated the uncertainty analysis to include an additional term representing uncertainty in the interpolation between transects. This is discussed in more detail in the response letter below. We have added a new Appendix, which details the error propagation procedure and underlying sources of uncertainty: "Appendix A: Uncertainty analysis for emission flux quantification."

Regarding verification of the assumptions used in the extrapolation: for the far flux curtain, uneven terrain and tall bushes posed hazards to the UAV, and the lowest measured transect was 6.5 m above the ground. These same obstacles also made the area beneath the far curtain inaccessible to ground vehicles. For the near curtain, the lowest transect was 2.5 m above the ground – the minimum clearance for the automated flights. Limited vehicle-based measurements were recorded for the near transect using a custom built closed-path TDLAS methane sensor similar to the open-path instrument in Norooz Oliaee et al. (2022). However, the air intake for that system was approximately 2 m above the ground and therefore offers limited value for verifying the extrapolation below the lowest UAV transect. The vehicle measured one transect along the road beneath the near curtain immediately following the UAV flight, recording a transect-integrated CH_4 mole fraction of 8.7 ppm·m. The transect-integrated CH_4 mole fraction used to extrapolate below the lowest transect (at 2.5 m) was 8.6 ± 3.7 ppm·m. Further comparisons with vehicle-based measurements are beyond the scope of this paper but are planned for future work.

A more detailed discussion on the accuracy of UAV-based wind measurements is required, given that wind is a critical parameter in mass-balance calculations.

We have added a new subsection to Methods titled "2.6 Onboard wind measurements," which describes the procedure for extracting the true wind speed and direction from onboard anemometer measurements. We have also added a new subsection to Results titled "3.3.1 Onboard wind measurements." This subsection contains the new Fig. 9 (see below) showing the raw and corrected wind measurements for the near curtain in the controlled-release. The corrected results are also compared with measurements from the stationary anemometer at the release point.

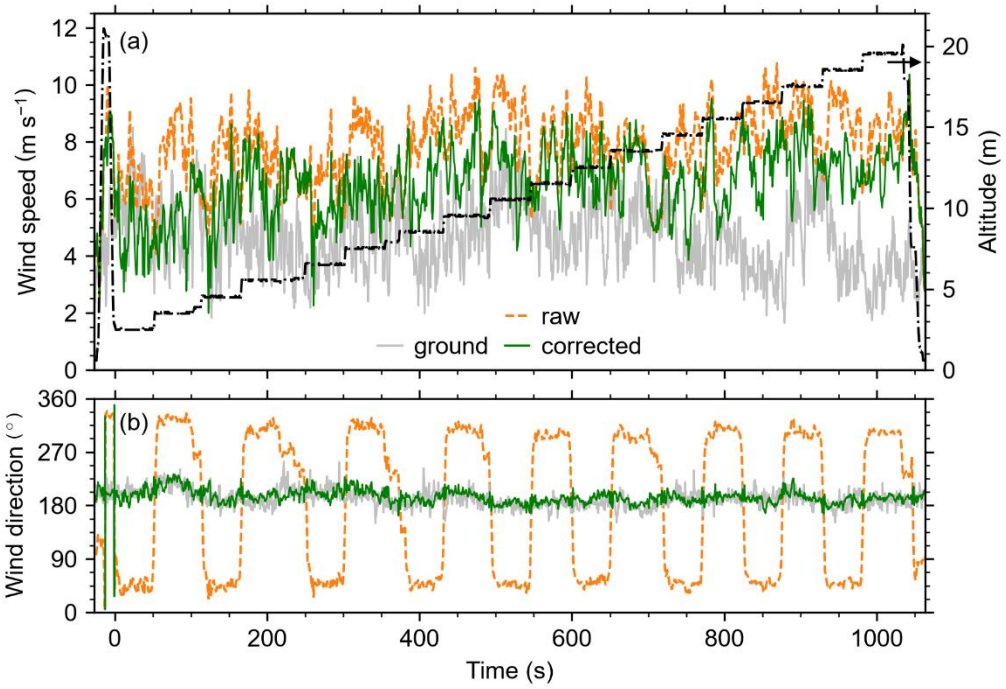

Figure 9. *Raw and corrected measurements of (a) wind speed (b) direction recorded by the onboard anemometer for the near curtain. Measurements from the stationary ground anemometer are shown for comparison. UAV height above takeoff is also shown in (a).*

The calibration and performance assessment of the spectrometer were carried out in the laboratory, which may not reflect real-world conditions. The authors should clarify potential impacts of environmental perturbations: changes in airflow through the MPC (due to UAV speed, wind direction, hovering), variations in pressure and temperature, and the effect of these factors on the non-linear calibration curve. Similarly, the potential dependence of measured fluxes on the true emission rate warrants discussion.

We agree with the reviewer that laboratory performance does not always reflect real-world conditions. To further characterize the instrument response when subjected to variations in temperature, pressure, humidity, and air flow, we have performed additional experiments and data analyses and made significant changes to the manuscript. These changes include a new subsection in Results titled: "3.2 Sensitivity to changing environmental conditions," which presents laboratory experiments in which the temperature and humidity were varied over time and for different methane mole fractions. We have also added a new subsection "3.3.3 In-flight stability and performance," which shows how the background methane mole fraction varies over time during a flight. Along with the methane background, we have plotted timeseries data for the 2*f* peak and trough positions, altitude, temperature, pressure, relative humidity, ground speed, yaw, pitch, roll, wind speed, and wind direction. We show that most of the baseline drift occurs during takeoff and landing (up to 5% variation), but the maximum drift observed while executing the curtain flight pattern is 2.5%.

Both the laboratory experiments and the in-flight observations are considered in the uncertainty budget for the flux estimation, which is now discussed in much greater detail, including the new Appendix: "Appendix A: Uncertainty analysis for emission flux quantification."

The manuscript does not sufficiently address the uncertainties introduced by the necessary interpolation across the vertical plume curtain. A more substantial dataset would be required to evaluate these effects robustly, which is not achievable within the reported 54-minute field campaign.

We agree with the reviewer that interpolation over the measured curtain introduces an important source of uncertainty in the emission rate estimate and that a larger set of controlled release experiments with statistical significance would be required to fully assess the magnitude of this uncertainty contribution – an undertaking that is beyond the scope of this paper. Bonne et al. (2024), Dooley et al. (2024), and Scheutz et al. (2025) have collectively performed at least 70 flights with their UAV-based methane sensors during controlled release experiments and have demonstrated emission flux quantification using very similar direct mass balance approaches where the integration is performed using either the trapezoid method (linear interpolation) or Reimann sums. Across 45 flights, Bonne et al. (2024) demonstrated that the direct mass balance prediction error ranged from -69% to 150% for all flights, and from -50% to 100% for 80% of the flights, relative to the actual release rate. Scheutz et al. (2025) published results from 12 controlled release flights and demonstrated predictions with a relative error in the range of -35.4% to 33.4% compared to the true rate. Neither Bonne et al. (2024) nor Scheutz et al. (2025) assigned uncertainty values to the predictions themselves. Dooley et al. (2024) attempted to estimate the uncertainty in their predicted flux rates by propagating the uncertainty associated with the measured parameters, without accounting for the uncertainty due to the interpolation. In five of eight reported flights, the true release rate fell within their reported 2σ error bars. For the remaining flights, they underestimated the release rate by up to 50%.

In our original manuscript, we followed a similar approach for uncertainty propagation to Dooley et al. (2024), going one step further by estimating uncertainty introduced by extrapolation below the lowest transect, which may be significant for emission sources that are close to the ground. In our revised manuscript, we have also attempted to estimate the uncertainty contribution due to vertical interpolation between transects in the flux curtain, using a leave-one-out cross-validation approach. The newly estimated 2σ error bars are 40% for the far flux curtain and 47% for the near curtain, which are broadly consistent with the expectations established by Bonne et al. (2024), Dooley et al. (2024), and Scheutz et al. (2025). The procedure for uncertainty estimation and propagation is described in detail in "Appendix A: Uncertainty analysis for emission flux quantification."

We have added a brief comparison to Bonne et al. (2024), Scheutz et al. (2025) in the text:

L. 563-566: "The reported 2σ error bounds correspond to relative uncertainties of 40% (far) and 47% (near). The true methane release rate, 0.48 kg h^{-1}, falls well within uncertainty for both estimated flux rates, differing by 8.8% for the far curtain and 1.6% for the near. For comparison, Bonne et al. (2024) applied a similar quantification method and demonstrated a prediction error ranging from -69% to 150% over 45 flights, and from -50% to 100% for 80% of the flights, relative to the actual release rate. Scheutz et al. (2025) published results from 12 controlled release flights and demonstrated predictions with a relative error in the range of -35.4% to 33.4% compared to the true rate."

The authors should also reconsider the title and abstract. The introduction suggests a focus on instrumentation, but the bulk text emphasizes flux estimation. Given that no substantive new instrumental development is presented, this contrast

weakens the paper's positioning. Furthermore, mass-balance flux estimation involves more than "just" UAV-based concentration measurements.

We thank the reviewer for their comments. We have revised the manuscript title:

"Ultra-Lightweight Mid-IR Methane Sensor for in-situ UAV-based Measurements: Design and Demonstration"

We have also revised the introduction to clarify that the paper presents a complete system for UAV-based mass-balance flux estimation:

L. 126-129: "We present the instrument's laboratory and field performance when deployed on a small enterprise-grade UAV, and evaluate the impact of variable environmental conditions. We also present a complete system for UAV mass-balance flux estimation including an on-board anemometer for wind measurements. The system's capacity to estimate emission rates from a methane point source is demonstrated in a controlled release experiment."

As described above, we have also expanded the discussion of the mass-balance flux estimations and added additional sections detailing the onboard wind measurements.

The reviewer's comment that "no substantive instrumental development is presented" highlights that the original text did not sufficiently explain the novelty of the sensor described in this work. The earlier publication referenced by the reviewer (Norooz Oliaee et al., 2022) relied on a longer multi-pass cell, a powerful computer, and a commercially available data acquisition board. Although both systems use an equivalent laser and photodetector, the sensor described in the present work is a compact, ultra-lightweight instrument built around entirely new hardware and electronics, including a smaller multi-pass cell and a custom-built data acquisition system. These substantial design changes reduced the instrument's size by approximately 84%, its weight by 75%, and its power consumption by 40% compared to the previously published instrument, resulting in one of the smallest and lightest methane spectrometers reported to date. In the revised manuscript, we have expanded on the discussion comparing the two instruments to more clearly highlight the similarities and key differences between this ultra-lightweight sensor and its larger predecessor. The revisions are shown below:

L. 6-8: "Weighing just 1.2 kg, including the dedicated battery, the stand-alone, power efficient instrument is 75% lighter than our previous design, making it one of the lightest methane sensors reported to date."

L. 111-112: "Compared to its predecessor, the new instrument is substantially smaller, lighter, and more power efficient, achieving a unique combination of high performance with an ultra-lightweight, compact design."

L. 168-170: "At room temperatures and in steady-state, the sensor package (including the SBC) consumes around 11 W of electrical power. For comparison, the previous version of this TDLAS methane sensor had a steady state power draw of around 18 W (Norooz Oliaee et al., 2022)."

L. 217-221: "The sensor package is compact and easily portable, with outer dimensions of 23.5 cm (L) × 12.5 cm (W) × 9.5 cm (H), approximately 84% smaller than the prior instrument (Norooz Oliaee et al., 2022). Including all electronics, batteries, and peripheral devices such as ambient condition (pressure, temperature, and relative humidity) sensors and a GPS receiver, the mass of the sensor package is just 1.2 kg, roughly one quarter that of its 5 kg predecessor (Norooz Oliaee et al., 2022)."

L. 581-582: "Compared with its predecessor, the new instrument is 84% smaller, 75% lighter, and consumes 40% less power."

Abstract: Technical details of the data acquisition system are not central to the key findings and can be removed. The authors should instead summarize the field-experiment results. The statement that the instrument "can be deployed to measure natural sources that would be undetectable for other methods" is too strong given that only a single suitable flight was analyzed. The authors should instead outline a realistic outlook, such as: "The instrument could be deployed in future controlled release experiments to validate its performance for detecting fugitive anthropogenic methane emissions (e.g., oil and gas infrastructure)."

We thank the reviewer for their suggestions. The revised abstract is below.

L. 1-16: "Uncrewed aerial vehicles (UAVs) offer versatile platforms for low-altitude (1 to 120 m) trace-gas measurements that can fill spatio-temporal measurement gaps between ground-based mobile platforms and conventional aircraft measurements. Small UAVs (under 25 kg) are easier to transport and typically face fewer regulatory restrictions than larger ones. However, they have significant payload limitations, underscoring the importance of developing lightweight, high-performance gas sensors for UAV deployment. In this work, we developed an ultra-lightweight methane sensor based on mid-infrared spectroscopy for precise, rapid in-situ measurements aboard small UAVs. Weighing just 1.2 kg, including the dedicated battery, the stand-alone, power efficient

instrument is 75% lighter than our previous design, making it one of the lightest methane sensors reported to date. The design is simple and compact, featuring a Herriott-type multi-pass cell in an open-path configuration. We report the sensor performance in detail in both laboratory experiments and field deployments, including the response to variable environmental conditions. The measurement precision for a 1 s averaging time is 3.7 ppb in the laboratory and 6.6 ppb in-flight. The 0.1 s in-flight precision, which is more suitable for monitoring rapidly varying methane from a fast-moving platform, is 26.5 ppb. We deployed the sensor in a controlled-release experiment with a methane point source emitting 0.48 kg h^{-1}. Using a direct mass balance flux quantification approach and wind measurements recorded by an on-board anemometer, estimated emissions were within 9% of the true emission rate. The results demonstrate the instrument's potential for in-situ measurement of fugitive emissions from anthropogenic and natural point sources. Further systematic controlled-release studies are needed to fully assess the detection probability and quantification accuracy of this UAV-based measurement system."

Additionally, we have a second manuscript in which we measured emissions from a naturally occurring geologic methane seep, including a comparison to the commercially available Aeris MIRA Strato sensor deployed on a second UAV system. That manuscript was concurrently under review and was recently accepted for publication in AMT (Bolek et al., 2026). As shown in that work, emission rate estimates were similar for both sensing platforms, on the order of 10 kg h^{-1}, further demonstrating our sensor's suitability to characterize emissions from point sources.

Methods:

The rationale for selecting WMS over DAS is not explained. The authors should briefly discuss the limiting factors for DAS in this context.

We thank the reviewer for highlighting this oversight. We have expanded on the text in the Introduction to explain the choice of WMS over DAS. The revised text is below:

L. 117-123: "Detection of the filtered and demodulated signal at harmonics of the modulation frequency enhances the signal-to-noise ratio and the measurement sensitivity as compared to DAS (Norooz Oliaee et al., 2022). The gas mole fraction is retrieved from the amplitude of the corresponding peak in the second harmonic spectrum. Beyond improved signal-to-noise, the implementation of WMS is simpler than DAS and more easily adapted to the ultra-lightweight embedded platform with its onboard single board computer (SBC). Conversely, the more complicated DAS fitting algorithms require more computational resources than WMS, which may necessitate a more powerful SBC or the use of a ground station to process the spectral data (Tuzson et al., 2020)."

The manuscript should clarify what quantity the analyzer measures. Greenhouse gas concentrations are typically reported as dry mole fractions—how was water-vapor effect corrected? Although the analyzer records H_2O, this was not shown or discussed.

The instrument measures the methane mole fraction – not the dry mole fraction. We have clarified the language in the manuscript to refer to 'mole fraction' specifically. We have also added a new subsection in Results titled: "3.2 Sensitivity to changing environmental conditions," which describes how nearby water lines affect the recorded methane mole fraction.

Flux estimation requires interpolation of measurements along the vertical direction. A description of the interpolation method is missing.

Linear interpolation is used between the horizontal transects. We have expanded on the relevant text in Section 2.7 to clarify the interpolation approach:

L. 298-303: "Following the trapezoid rule, linear interpolation is used when integrating between transects—both measured and extrapolated—in Eq. 5. This direct interpolation approach is suited to datasets characterized by dense sampling across the measurement plane (Bonne et al., 2024; Bolek et al., 2026; Scheutz et al., 2025; Dooley et al., 2024). More complex statistical interpolation approaches such as Kriging have also been proposed (Morales et al., 2022; Andersen et al., 2021), and may be more suitable than direct interpolation for sparse datasets."

Specific Comments

L90: Remove "free space" before "laser".

"Free space" has been removed.

L91: Specify the tuning rate used for the spectral scan.

The tuning rate was originally specified in the "Onboard signal generation, acquisition, and processing section." We have added an additional reference to the tuning rate here:

L. 132-135: "We use a collimated GaSb-based distributed feedback (DFB) diode laser (NL3270-TL, Norcada, Canada) with a specified operating temperature range from -20 to 40 °C. The laser wavelength is 3270.4 nm at 7 °C when the injection current is 130 mA. During operation, the tuning rate is approximately 20 pm mA^{-1}, as discussed in Section 2.3"

In Fig. 2c, replace channel number with optical frequency (cm^{-1}).

We added a secondary *x*-axis to Fig. 2(c) to show the optical frequency in cm^{-1}.

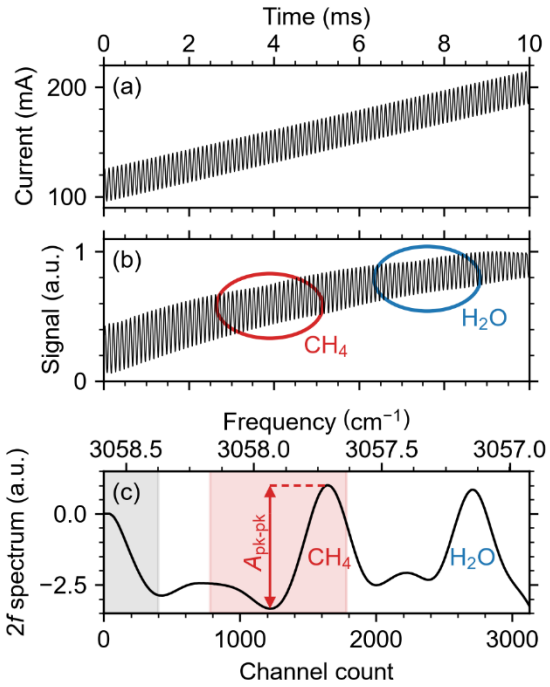

Figure 2. *(a) Laser injection current ramp and 10 kHz modulation over one sawtooth period. (b) Corresponding normalized detector signal observed under ambient measurement conditions. (c) Demodulated second harmonic spectrum, normalized. Absorption features due to CH_4 and H_2O are indicated in (b, c). The gray shaded region in (c) spanning channels 0 to 400 contains the initial response of the low pass filter and does not indicate absorption. The red shaded region covering the CH_4 peak indicates the predefined bounds used to identify the peak-to-peak amplitude.*

L96/98: Remove unnecessary trailing zeros.

Trailing zeros have been removed.

L106: Remove "has no moving part".

This text describing the optical alignment procedure has been revised and moved to "Section 2.1: Optical Assembly". The revised text reads:

L. 148-154: "Laser pre-alignment is achieved using a mounting plate machined at the desired injection angle. The optical alignment is fine-tuned during the assembly procedure using shims and split lock washers to correct deviations in the laser pointing angle. The split lock washers provide small angular adjustment capability, while slightly over-sized mounting holes for the laser heat sink and OAPM allow limited translational freedom. Final alignment was achieved by measuring the laser pointing angle, applying the required corrections, and making small translational and angular adjustments to maximize the detector signal observed on an oscilloscope. The number and approximate positions of the reflected spots are confirmed by systematically blocking the laser beam."

L110: Compare the 1.2 kg sensor package with the MIRA Pico regarding weight, precision, stability, and response time.

We have added an overview of similar sensors that have been deployed on UAVs, including the MIRA Pico, to the introduction:

L. 80-107: "Several methane sensing instruments based on tunable diode laser absorption spectroscopy (TDLAS) have been developed for UAVs. Nathan et al. (2015) developed an open-path sensor employing a near-infrared (1651 nm) diode laser light

source in wavelength modulation spectroscopy (WMS) mode and deployed it on an electric fixed-wing model aircraft with a wing span of 3 m. The sensor weighed 3.1 kg with a 1 Hz precision of 100 ppb and a power consumption of 25 W. Golston et al. (2017) used a mid-IR diode laser (3270 nm) in WMS mode for their open-path instruments. Two versions of the sensor were reported for fixed-wing and rotary-wing UAVs weighing 4.7 kg and 1.6 kg, inclusive of batteries, with reported precisions of 5 ppb and 10 ppb at 1 Hz, respectively. The sensor power consumption was reported to be 30 W. Bonne et al. (2024) also used mid-IR open-path TDLAS for their combined CH_4 and CO_2 sensor. The sensor employed direct absorption spectroscopy (DAS), weighed 1.4 kg (not including dedicated batteries), had a 1 Hz precision of 10 ppb for CH_4 detection, and consumed 8 to 15 W of power. Smith et al. (2023) report open- and closed-path TDLAS instruments that were developed for fixed-wing and rotary-wing UAVs. The sensors weigh 0.6 and 0.85 kg with reported 1 Hz precisions of 40 ppb and 164 ppb, respectively. Shah et al. (2020) developed a closed-path near-IR TDLAS instrument that employs the off-axis integrated cavity output spectroscopy (ICOS) sensing technique. The sensor weighs 3.4 kg, has a 1 Hz precision of 2.2 ppb, and a power consumption of 32 W. Commercially available MIRA Pico and MIRA Strato mid-IR sensors from Aeris Technologies (USA) have also been deployed on UAVs (Dooley et al., 2024; Bolek et al., 2024, 2026). These sensors employ DAS, weigh 3 kg and 2 kg, respectively, and have reported 1 Hz precisions of <1 ppb and <2 ppb. Their steady state power consumption is in the range of 15-18 W.

Gas sensors based on quantum cascade laser absorption spectroscopy (QCLAS) have also been developed for aerial platforms (D'Amato et al. 2025; Tuzson et al. (2020). Quantum cascade lasers (QCLs) extend further into the mid-infrared wavelength range than tunable diode lasers (TDLs), which is advantageous for gas spectroscopy, where many gases exhibit the strongest absorbance in the mid-infrared (3 to 20 µm) (D'Amato et al., 2025). For methane, however, the strongest absorbance is found in the ν_3 fundamental C-H stretching mode near 3.3 µm (Dang-Nhu et al., 1979), which is accessible to both QCLs and TDLs. QCLs are typically more expensive than TDLs and have much higher power consumption when operating in continuous-wave mode (D'Amato et al., 2025). As such, TDLs are a more popular choice for methane gas spectroscopy than QCLs. One notable lightweight QCLAS methane sensor that was designed for UAV applications was developed by Tuzson et al. (2020). This instrument targeted methane's mid-infrared absorption line at 7.83 µm. The sensor weighed 2.1 kg (including the battery) and had a reported 1 Hz precision of 1.1 ppb. Its power consumption was 18 W, enabled using an intermittent continuous-wave laser driving approach."

We also compare back to these instruments in the Methods and Results sections. Relevant text is below:

L. 221-224: "As one of the lightest methane gas spectrometers developed to date, the instrument is well within the payload limits of many small consumer- or enterprise-grade UAVs such as the DJI Matrice 300 RTK used in this study, allowing for simultaneous deployment of an on-board anemometer system on a highly portable measurement platform, as described in Section 2.5."

L. 357-360: "The 1 s averaging times (in-flight precision: 6.6 ppb; laboratory precision: 3.7 ppb) represent a useful metric for comparison to other lightweight UAV sensors. Though other instruments offer slightly smaller 1 s precisions in the range of 1-5 ppb, to our knowledge the ultra-lightweight sensor presented here offers the best 1 s precision for a sub-2 kg methane sensor reported to date."

L. 504-507: "Drift is known to affect other UAV-borne sensors including commercial instruments such as the Aeris MIRA Pico and Strato sensors (Dooley et al., 2024; Bolek et al., 2026). Notably, Dooley et al., (2024) showed a systematic drift of roughly 250 ppb over a 20-minute UAV flight for a MIRA Pico sensor."

Additionally, a qualitative comparison of the sensor response for the ultra-lightweight instrument presented here and the Aeris Strato sensor can be found in Bolek et al. (2026).

L117: Discuss the impact of rapid ambient-temperature changes on detector responsivity.

The following text has been added:

L. 163-165: "Under active airflow, the temperatures of both laser and detector typically stabilize within 10 minutes. A similar stabilization period is required after rapid, substantial changes in ambient temperature. During UAV flight, the laser temperature is maintained to within ±0.1 °C, which corresponds to a wavelength stability of ±0.028 nm (±0.026 cm^{-1})."

The impact of rapid ambient-temperature changes on the methane sensor is also discussed in the newly added subsection "3.2 Sensitivity to changing environmental conditions," which includes new results from a laboratory experiment where the temperature was rapidly varied over a range of approximately 8 °C. An excerpt from the revised manuscript is below:

L. 387-393: "Although the TECs that control the temperatures of the laser and photodetector can adapt to gradual variations in ambient temperature and maintain stable performance across a wide temperature range, sudden shifts in ambient temperature may cause temporary instability. The impact of rapid changes in temperature in the range of 19.7 to 27.5 °C is shown in Fig. 6. The

timeseries data corresponds to the native 100 Hz sensor output. To clearly illustrate the effect of the rapid temperature variation, the 60 s moving average is also shown, indicated by the black dashed line. Oscillatory behavior is observed in the sensor signal immediately after each abrupt temperature change. Over the entire experiment, the 60 s moving average varies by 4.1%."

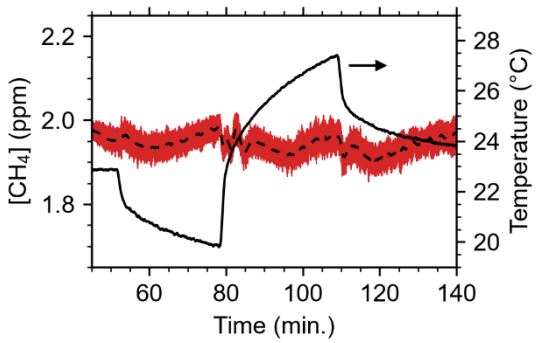

Figure 6. *100 Hz time series for the recorded methane mole fraction while the temperature of the calibration enclosure was rapidly varied (red). The dashed line indicates the 60 s moving average. Temperature is shown on the right-hand axis.*

L130: The timing-accuracy statement is redundant, given that bandwidth was already defined.

The sentence containing this statement has been removed.

L137: Clarify why a modulation current of 15 mA was chosen. The modulation index appears sub-optimal in Fig. 2c.

We thank the reviewer for this comment. The modulation current of 15 mA was selected empirically to maximise the 2*f* signal amplitude while avoiding excessing over-modulation that would result in distortion and broadening of the spectral features in the demodulated spectrum. We agree that the modulation index is not fully optimised in Figure 2c. However, a systematic optimisation of the modulation amplitude was not the objective. Instead, a modulation level was chosen to balance signal strength and spectral fidelity. It is also important to note that the appearance of the demodulated spectra depends not only on the modulation index but also on the lock-in amplifier settings, particularly the low-pass filter time constant and detection phase. Therefore, the apparent sub-optimality in Fig. 2(c) reflects the overall effect of modulation amplitude, filter and demodulation phase effects. To clarify this point, we have revised the manuscript to explicitly state that the modulation amplitude was selected empirically rather than reflecting an optimized modulation index. The revised text now reads:

L. 188-190: "The amplitude of the modulation signal was chosen empirically to increase the second harmonic signal amplitude while avoiding excessive over-modulation and does not reflect the well-known optimum modulation index ($m \approx 2.2$) (Rieker et al., 2009; Reid and Labrie, 1981)."

L237: Remove "per minute" and "an in line".

The revised sentence reads:

L. 307-308: "The calibration gas flow was maintained near 10 L min^{-1}."

L245: Discuss the sensor response to sudden changes in pressure/flow/temperature.

This comment has been addressed through the addition of two new subsections in Results. Subsection "3.2 Sensitivity to changing environmental conditions," discusses the effect of ambient-temperature changes and demonstrates those effects through laboratory experiments that vary the ambient temperature. Subsection "3.3.3 In-flight stability and performance," shows how the background methane mole fraction varies over time during flight, including takeoff and landing. Along with the methane background, we have plotted timeseries data for pressure, which varies rapidly with altitude, as well as the UAV flight data (altitude, ground speed, heading, pitch, and roll) and the wind speed and direction, which all contribute to changes in air flow experienced by the onboard sensor. An excerpt from the new Section 3.3.3 is below:

L. 524-531: "When comparing variations in the background methane mole fraction to the other timeseries datasets shown in Fig. 11, no apparent correlations are observed. Though other airborne spectroscopic gas analyzers have been shown to be strongly influenced by rapid changes in the movement of the aircraft (Ort et al., 2024), the open-path instrument does not appear to be affected by rapid in-flight variations in the UAV ground speed, yaw, pitch, or roll. Likewise, change in wind speed and direction do not appear to influence the instrument response. The observed drift is therefore attributed primarily to changes in temperature, pressure, relative humidity, and air flow (during takeoff and landing), which are known to affect the recorded mole fractions. More

accurate and comprehensive onboard measurements of environmental conditions are needed to discern and mitigate the effects that impact the sensor's reading."

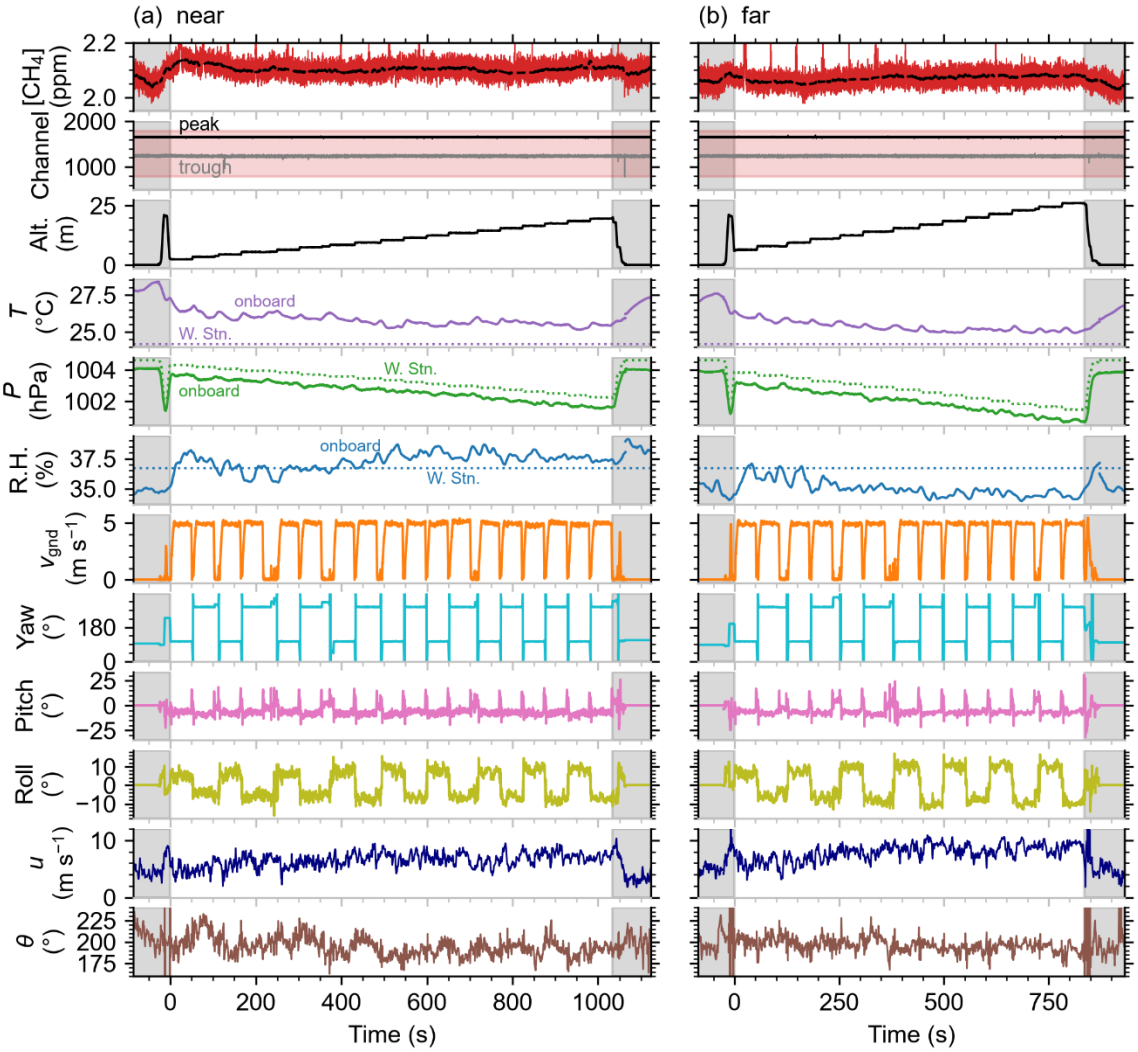

Figure 11. *Collection of parameters recorded over time for controlled-release (a) near and (b) far curtain flights. In order from top to bottom, the parameters are: methane mole fraction, 2f peak and trough channel numbers, altitude (Alt.), temperature (T), pressure (P), relative humidity (R.H.), ground speed (vgnd), heading (yaw), pitch, roll, wind speed (u), and wind direction (θ). The gray shaded bars at the beginning and end of each timeseries indicate data that falls outside of the defined flux curtain, including UAV takeoff and landing. The methane mole fraction scale is adjusted to emphasize the slowly varying baseline, displaying both the 10 Hz time series and the 5.8-second moving average of the background (black dashed line). The red shaded region in the peak and trough channel plot indicates the search bounds defined in Fig. 2. T, P, and R.H. measurements are shown for both the onboard sensor (10-second moving average) and average values from a local weather station (W. Stn.). Wind speed and direction were from the onboard anemometer.*

L249: The calibration uncertainties (e.g., ~0.45 ppm at 2.5 ppm CH_4) are substantial. More detailed assessment at ambient CH_4 levels is needed.

We have added a new subplot in Fig. 3 showing the calibration fit relative residuals $([CH_4]-[CH_4]_{fit})/[CH_4]_{fit}$ and the relative 1σ uncertainty bounds and the 95% confidence interval on the fit, which were computed using the full covariance matrix. At 2.5 ppm, the 1σ error bound is 0.5% (12.5 ppb) and the 95% confidence bound on the fit is ~1.4% (35 ppb). Please note that we have also replaced the data shown in Fig. 3 with a calibration that was benchmarked against a newly acquired LICOR LI-7810 gas analyzer, providing a much more reliable reference. This includes additional measurement points at mole fractions <5 ppm, and an inset that shows the calibration curve to be nearly linear in this range. The new figure is below:

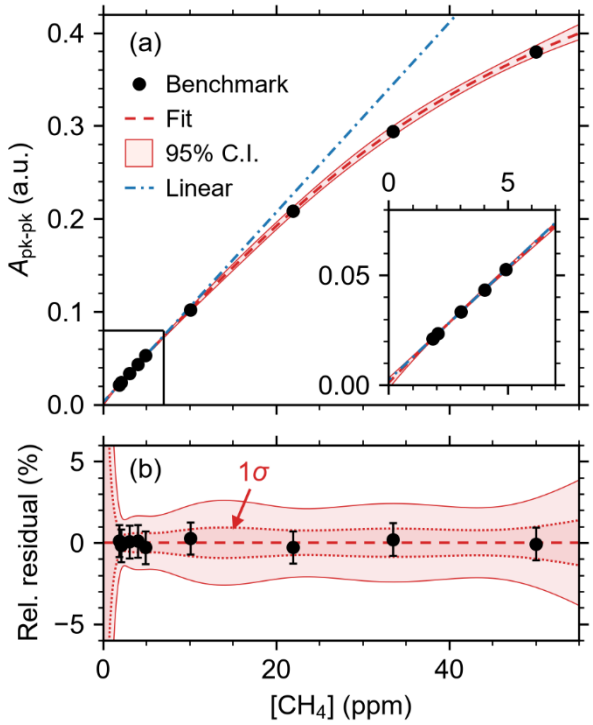

Figure 3. *(a) WMS 2f peak-to-peak amplitude as a function of methane mole fraction measured by benchmark instrument (LI-7810). Fit to Eq. 7 is shown with 95% confidence interval. For reference, a linear fit to the data points below 10 ppm is also shown. Inset shows expanded view of data points up to 5 ppm. (b) Relative residuals ($[CH4] - [CH4]_{fit}$)/$[CH4]_{fit}$, where error bars indicate 1% uncertainties on the methane mole fraction. The 1σ standard error on the fit is also shown.*

We also evaluated the ultra-lightweight (ULW) sensor response for rapidly varying CH_4 mole fractions in the range of ~2.2-3.2 ppm and compared the result to the commercial Aeris MIRA Pico and LICOR 7810 sensors (Fig. R1). The ULW sensor was placed in the calibration enclosure adjacent to a gas inlet shared by the Aeris MIRA Pico and the LICOR 7810. Building compressed air with a slightly elevated methane mole fraction flowed through the enclosure at a rate of 15 L min^{-1}. Small amounts of 8004 ppm CH_4 in synthetic air were injected, generating abrupt changes in the methane mole fraction. The ULW sensor and the Aeris MIRA Pico were both calibrated against the LICOR 7810 in the range of ~2-6 ppm. The data shown for the ULW sensor corresponds to its intrinsic 100 Hz data rate. There was good agreement between the results reported by all three sensors over the 25-minute measurement period. Fig. R1(b) shows a more detailed view of the step at around 630 s, illustrating the difference in response time between the three instruments. The sharp spike recorded by the ULW sensor at each step is correlated with the injection of 8004 ppm methane, before it fully mixes with the gas in the enclosure.

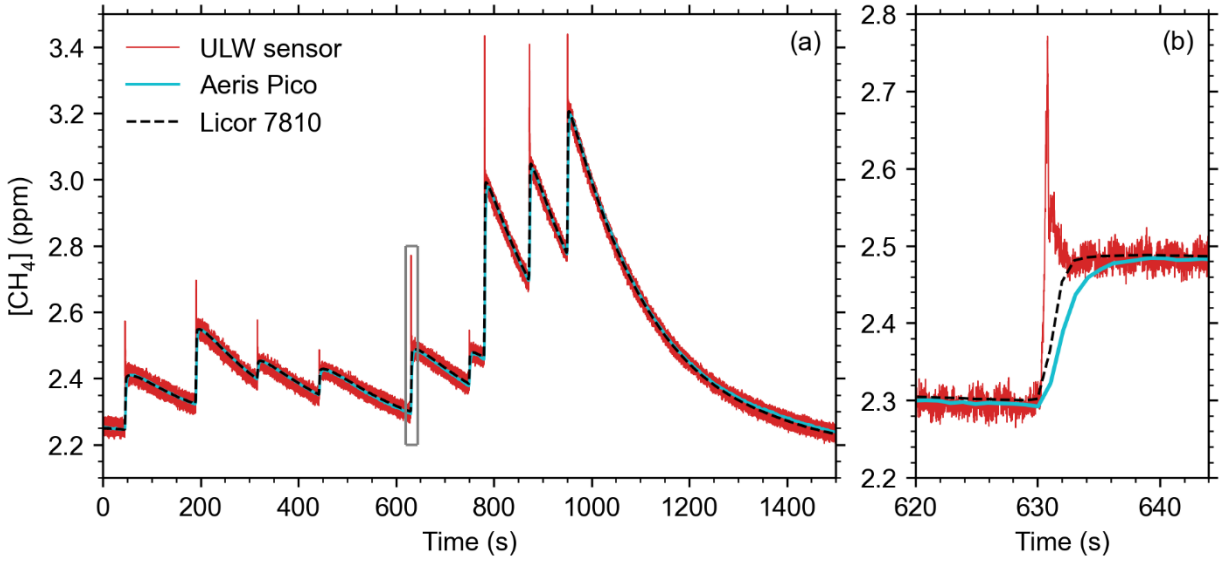

Fig. R1 (a) CH_4 mole fraction timeseries over 25-minute measurement period for the ULW sensor and commercial Aeris MIRA Pico and Licor 7810 sensors. (b) Expanded view of the region indicated by the gray box in (a).

L259: Additional in-flight noise is attributed to inductive effects. How does this scale without real-time data streaming? How can it be mitigated? Is this typical for UAV-mounted spectrometers?

We thank the reviewer for their question. Laboratory tests show that the on-board radio used for real-time data streaming increases the standard deviation of the raw sensor signal by at least a factor of 3.3. In-flight noise beyond this level is likely attributable to the UAV deployment, including vibrations and further inductive interference from UAV communication links.

Laboratory experiments indicated that the radio's noise contribution is primarily inductive rather than conductive in nature. The results suggest that a Faraday-cage-style protective housing could help to mitigate this effect. Increased physical separation between the sensor and the radio may also reduce its noise contribution, as discussed in the text:

L. 343-344: "It may be possible to reduce this noise component by implementing design modifications such as a Faraday cage to mitigate electromagnetic interferences."

We have not seen this effect discussed in the literature for other UAV-mounted spectrometers. Future work will involve more in-depth investigation of sources of noise and solutions for their mitigation.

L269: Rephrase "flat region in the laboratory Allan measurements".

Revised sentence reads:

L. 345-348: "The in-lab Allan-Werle deviation below 0.1 s averaging time is affected by a quasi-periodic noise signature for which averaging does not initially improve the measurement precision, appearing as random-walk or correlated noise in the Allan-Werle plot. Though the root cause is still under investigation, the effect is likely induced by correlated mechanical or electrical noise (Röder et al., 2024; Gan et al., 2026). For the in-flight data, there is a deviation from the $\sqrt{1/\tau}$ white noise behavior observed for averaging times between 0.1 and 1 s that may be due to optical fringe effects that are not observed in the laboratory data (Werle, 2011)."

L270: Specify the hardware and software filters used, including 3 dB roll-off frequencies.

We thank the reviewer for this comment. We have revised Section "2.3 Onboard signal generation, acquisition, and processing" to include a more detailed description of the filter architecture:

L. 177-178: "For reference, the DAC and ADC have simple passive RC filters at their input and output with 3 dB bandwidths of 32.8 kHz and 48.2 kHz, respectively."

L. 191-192: "The photocurrent signal from the photodetector is converted to a voltage using a custom two-stage transimpedance amplifier (TIA) with a 3 dB bandwidth of 141 kHz."

L. 197-198: "… a numerical fourth-order low-pass filter with a −3 dB cutoff frequency of 561 Hz is applied, implemented as two cascaded second-order biquad sections, each with a cutoff frequency of 700 Hz."

L271: Reconsider the wording of "limited or flattened noise".

This has been revised. The excerpt from lines 345-348 is shown above.

Fig. 4: Strong filtering is observed here but not in Norooz Oliaee et al. (2022, Fig. 6). The reported 1-s precision is also four times worse despite filtering. This discrepancy needs discussion.

We thank the reviewer for their comment. The sensor presented in this paper employs a more compact multi-pass cell with a shorter path length and completely different hardware and electronics from its predecessor. This enabled development of a very compact, lightweight instrument – which is ideal for UAV deployment. The reduced precision is a trade-off that will limit the detection of very small methane enhancements (< 5 ppb).

L280: To avoid confusion, use consistent units (L min^{-1} instead of introducing SLPM).

Revised sentences reads:

L. 429-430: "…12 standard L min^{-1} (20 °C and 1013.25 hPa)…"

L294: The UAV wind speed is sampled at 2 Hz while concentration data are at 10 Hz. Explain the motivation for these differing sampling rates.

We thank the reviewer for their question. We acknowledge that the selection of a 2 Hz data rate for wind measurements was shortsighted, and a faster data rate of at least 10 Hz would have been preferable. This is discussed in the new subsection under Results titled "3.3.1 Onboard wind measurements." The relevant text follows:

L. 469-472: "Brief instabilities in the wind speed and direction recorded by the onboard anemometer at takeoff and landing are attributed primarily to interpolation of the 2 Hz wind data, as the data rate was slow compared to the rapid movements of the UAV. We expect that a faster data rate of at least 10 Hz would improve the wind measurement stability during takeoff and landing and improve measurement accuracy by removing the requirement to interpolate."

L305: Clarify what "very low" refers to regarding the 0.5 kg h^{-1} emission rate.

We thank the reviewer for this comment. We have now clarified what we mean by "very low." The revised text is below:

L. 444-445: "…demonstrating detection at a methane emission rate <0.5 kg h^{-1}, which is below the limit of detection for most conventional aircraft surveys (El Abbadi et al., 2024; Duren et al., 2019; Donahue et al., 2026)."

References:

Andersen, T., Vinkovic, K., de Vries, M., Kers, B., Necki, J., Swolkien, J., Roiger, A., Peters, W., and Chen, H.: Quantifying methane emissions from coal mining ventilation shafts using an unmanned aerial vehicle (UAV)-based active AirCore system, Atmospheric Environment: X, 12, https://doi.org/10.1016/j.aeaoa.2021.100135, 2021.

Bolek, A., Heimann, M., and Göckede, M.: UAV-based in situ measurements of CO2 and CH4 fluxes over complex natural ecosystems, Atmospheric Measurement Techniques, 17, 5619–5636, https://doi.org/10.5194/amt-17-5619-2024, 2024.

Bolek, A., Beattie, M. N., Norooz Oliaee, J., MacLeod, R., Skeeter, J., Morse, P., Heimann, M., and Göckede, M.: Application of UAV-based methods for quantifying methane point source emissions over an Arctic geological seep, Atmospheric Measurement Techniques, 19, 3983–3998, https://doi.org/10.5194/amt-19-3983-2026, 2026.

Bonne, J. L., Donnat, L., Albora, G., Burgalat, J., Chauvin, N., Combaz, D., Cousin, J., Decarpenterie, T., Duclaux, O., Dumelié, N., Galas, N., Juery, C., Parent, F., Pineau, F., Maunoury, A., Ventre, O., Bénassy, M. F., and Joly, L.: A measurement system for CO2 and CH4 emissions quantification of industrial sites using a new in situ concentration sensor operated on board uncrewed aircraft vehicles, Atmospheric Measurement Techniques, 17, 4471–4491, https://doi.org/10.5194/amt-17-4471-2024, 2024.

Dang-Nhu, M., Pine, A. S., and Robiette, A. G.: Spectral Intensities in the v3 Bands of 12CH4, and 13CH4, Journal of Molecular Spectroscopy, 77, 57–68, 1979.

Donahue, C. P., Oberoi, K., Dillon, J. W., Hengst, V., Kennedy, B., Kearney, W., Lennox, J., Rehbein, E., Sykes, R., Dudiak, C. D., Altamura, D. T., Doherty, G., Roos, P. A., Brasseur, J. K., and Thorpe, M. J.: Aerial LiDAR-Based, Source-Resolved Methane Emissions Inventory: Permian Basin Case Study for Benchmarking U.S. Emissions, Environmental Science & Technology, 60, 13 968–13 979, https://doi.org/10.1021/acs.est.5c15184, 2026.

Dooley, J. F., Minschwaner, K., Dubey, M. K., Abbadi, S. H. E., Sherwin, E. D., Meyer, A. G., Follansbee, E., and Lee, J. E.: A new aerial approach for quantifying and attributing methane emissions: Implementation and validation, Atmospheric Measurement Techniques, 17, 5091–5111, https://doi.org/10.5194/amt-17-5091-2024, 2024.

Duren, R. M., Thorpe, A. K., Foster, K. T., Rafiq, T., Hopkins, F. M., Yadav, V., Bue, B. D., Thompson, D. R., Conley, S., Colombi, N. K., Frankenberg, C., McCubbin, I. B., Eastwood, M. L., Falk, M., Herner, J. D., Croes, B. E., Green, R. O., and Miller, C. E.: California's methane super-emitters, Nature, 575, 180–184, https://doi.org/10.1038/s41586-019-1720-3, 2019.

D'Amato, F., Barucci, M., Bianchini, G., and Viciani, S.: Quantum cascade laser (QCL) in airborne atmospheric measurements: A review [Invited], Optics Express, 33, 22 745, https://doi.org/10.1364/oe.558437, 2025.

El Abbadi, S. H., Chen, Z., Burdeau, P. M., Rutherford, J. S., Chen, Y., Zhang, Z., Sherwin, E. D., and Brandt, A. R.: Technological Maturity of Aircraft-Based Methane Sensing for Greenhouse Gas Mitigation, Environmental Science and Technology, 58, 9591–9600, https://doi.org/10.1021/acs.est.4c02439, 2024.

Gan, Q., Feng, Z., Zhang, D., Ma, S., Yang, X., and Yin, X.: High-Flow-Rate Trace Formaldehyde Detection Based on Ultraviolet Photoacoustic Spectroscopy Using a Long Resonant Photoacoustic Cell, Sensors, 26, https://doi.org/10.3390/s26051410, 2026.

Golston, L. M., Tao, L., Brosy, C., Schäfer, K., Wolf, B., McSpiritt, J., Buchholz, B., Caulton, D. R., Pan, D., Zondlo, M. A., Yoel, D., Kunstmann, H., and McGregor, M.: Lightweight mid-infrared methane sensor for unmanned aerial systems, Applied Physics B: Lasers and Optics, 123, https://doi.org/10.1007/s00340-017-6735-6, 2017.

Morales, R., Ravelid, J., Vinkovic, K., Korbe´n, P., Tuzson, B., Emmenegger, L., Chen, H., Schmidt, M., Humbel, S., and Brunner, D.: Controlled-release experiment to investigate uncertainties in UAV-based emission quantification for methane point sources, Atmospheric Measurement Techniques, 15, 2177–2198, https://doi.org/10.5194/amt-15-2177-2022, 2022.

Nathan, B. J., Golston, L. M., O'Brien, A. S., Ross, K., Harrison, W. A., Tao, L., Lary, D. J., Johnson, D. R., Covington, A. N., Clark, N. N., and Zondlo, M. A.: Near-Field Characterization of Methane Emission Variability from a Compressor Station Using a Model Aircraft, Environmental Science and Technology, 49, 7896–7903, https://doi.org/10.1021/acs.est.5b00705, 2015.

Norooz Oliaee, J., Sabourin, N. A., Festa-Bianchet, S. A., Gupta, J. A., Johnson, M. R., Thomson, K. A., Smallwood, G. J., and Lobo, P.: Development of a Sub-ppb Resolution Methane Sensor Using a GaSb-Based DFB Diode Laser near 3270 nm for Fugitive Emission Measurement, ACS Sensors, 7, 564–572, https://doi.org/10.1021/acssensors.1c02444, 2022.

Ort, L., Röder, L. L., Parchatka, U., Königstedt, R., Crowley, D., Kunz, F., Wittkowski, R., Lelieveld, J., and Fischer, H.: In-flight characterization of a compact airborne quantum cascade laser absorption spectrometer, Atmospheric Measurement Techniques, 17, 3553–3565, https://doi.org/10.5194/amt-17-3553-2024, 2024.

Reid, J. and Labrie, D.: Second-Harmonic Detection with Tunable Diode Lasers-Comparison of Experiment and Theory*, Appl. Phys. B, 26, 203–210, 1981.

Rieker, G. B., Jeffries, J. B., and Hanson, R. K.: Calibration-free wavelength-modulation spectroscopy for measurements of gas temperature and concentration in harsh environments, Applied Optics, 48, 5546–5560, 2009.

Röder, L. L., Ort, L., Lelieveld, J., and Fischer, H.: Quantitative analysis of temporal stability and instrument performance during field experiments of an airborne QCLAS via Allan–Werle-plots, Applied Physics B: Lasers and Optics, 130, https://doi.org/10.1007/s00340-024-08254-5, 2024.

Scheutz, C., Knudsen, J. E., Vechi, N. T., and Knudsen, J.: Validation and demonstration of a drone-based method for quantifying fugitive methane emissions, Journal of Environmental Management, 373, https://doi.org/10.1016/j.jenvman.2024.123467, 2025.

Shah, A., Pitt, J. R., Ricketts, H., Leen, J. B., Williams, P. I., Kabbabe, K., Gallagher, M. W., and Allen, G.: Testing the near-field Gaussian plume inversion flux quantification technique using unmanned aerial vehicle sampling, Atmospheric Measurement Techniques, 13, 1467–1484, https://doi.org/10.5194/amt-13-1467-2020, 2020.820

Shaw, J. T., Shah, A., Yong, H., and Allen, G.: Methods for quantifying methane emissions using unmanned aerial vehicles: A review, https://doi.org/10.1098/rsta.2020.0450, 2021.

Smith, B. J., Buckingham, S., Touzel, D. F., Corbett, A. M., and Tavner, C.: Development of Methods for Top-Down Methane Emission Measurements of Oil and Gas Facilities in an Offshore Environment Using a Miniature Methane Spectrometer and Long-Endurance Uncrewed Aerial System, in: SPE Production & Operations, vol. 565, pp. 565–577, Society of Petroleum Engineers, http://onepetro.org/PO/article-pdf/38/04/565/3309279/spe-206181-pa.pdf/1, 2023.

Tuzson, B., Graf, M., Ravelid, J., Scheidegger, P., Kupferschmid, A., Looser, H., Morales, R. P., and Emmenegger, L.: A compact QCL spectrometer for mobile, high-precision methane sensing aboard drones, Atmospheric Measurement Techniques, 13, 4715–4726, https://doi.org/10.5194/amt-13-4715-2020, 2020.

Werle, P.: Accuracy and precision of laser spectrometers for trace gas sensing in the presence of optical fringes and atmospheric turbulence, Applied Physics B: Lasers and Optics, 102, 313–329, https://doi.org/10.1007/s00340-010-4165-9, 2011.